

# Synthesis of Nanoflower like BTCA Doped Fe<sub>3</sub>O<sub>4</sub> /PANI Nanocomposites via Micelle Assisted Method

D. Rama Devi<sup>1</sup>, Y. Pavan Kumar<sup>2</sup>, K. Basavaiah<sup>3</sup>

<sup>1</sup>A.U. College of Pharmaceutical Sciences, Andhra University, A.P., India – 530003

<sup>2,3</sup>Department of Inorganic & Analytical Chemistry, Andhra University, A.P., India - 530003

**Abstract:** *Magnetic nanocomposites of benzene tetracarboxylic acid (BTCA) doped polyaniline (PANI) and magnetite nanoparticles (Fe<sub>3</sub>O<sub>4</sub> NPs) have been prepared by modified co-precipitation cum chemical oxidative polymerization method using ammonium persulphate as oxidant in the presence of organic carboxylic acid. The organic carboxylic acid can act as both dopant as well as surfactant for synthesis of PANI nanostructures. As synthesized BTCA doped PANI / Fe<sub>3</sub>O<sub>4</sub> nanocomposites have been characterized by X-ray diffraction, UV-visible spectroscopy, Fourier transform infrared spectroscopy, scanning electron microscopy, vibrating sampling magnetometer (VSM) and thermogravimetry analysis (TGA). Spectroscopic results indicated that the successful synthesis of BTCA doped PANI / Fe<sub>3</sub>O<sub>4</sub>. The morphology of nanocomposite was found to be dependent on the molar ratios of monomer to organic carboxylic acid. The VSM results reveal the superparamagnetic behaviour of PANI / Fe<sub>3</sub>O<sub>4</sub> nanocomposites.*

**Keywords:** Magnetic nanocomposites, Polyaniline, Magnetite Nanoparticles, Self-assembly

## 1. Introduction

The magnetic nanocomposites of intrinsic conducting polymer (ICP) and magnetite nanoparticles (Fe<sub>3</sub>O<sub>4</sub> NPs) have significant potential to allow the design of functional devices due to low density, high hardness, structural diversity, and improved electromagnetic properties to those of pure conducting polymers [1]. More recently, the magnetic nanocomposites based on polyaniline (PANI) and Fe<sub>3</sub>O<sub>4</sub> NPs have emerged as promising candidates for technological applications such as catalysis, EMI shielding, biomedical, anti-biofouling, electromagnetic device and immunity assay [2-4]. Most of these applications are gained importance due to a hybrid structural and functional combination between the conducting PANI and magnetic Fe<sub>3</sub>O<sub>4</sub> and also unique properties such as low toxicity, high saturation magnetization and biocompatibility of magnetic Fe<sub>3</sub>O<sub>4</sub> [5]. All these technological applications require the Fe<sub>3</sub>O<sub>4</sub> NPs to be uniform particle size without any aggregation and well dispersed in aqueous medium. However, Fe<sub>3</sub>O<sub>4</sub> NPs can tend to aggregate due to high surface to volume ratio, strong magnetic dipole-dipole interaction and Vander Waal's attractive forces among the Fe<sub>3</sub>O<sub>4</sub> NPs and hence they exhibit poor magnetic properties and low dispersibility. In view of this, the various approaches have been developed to prepare the aggregate free superparamagnetic Fe<sub>3</sub>O<sub>4</sub> NPs in nanocomposites by using various capping agents such as inorganic metals, metal oxides, surfactants and polymers. The capping agents not only arrest the aggregation of Fe<sub>3</sub>O<sub>4</sub> NPs but also provide a useful platform for desired technological applications via functionalization.

Numerous synthesis approaches have been reported for preparation of PANI/Fe<sub>3</sub>O<sub>4</sub> nanocomposites such as synthesis of PANI in the presence of Fe<sub>3</sub>O<sub>4</sub> NPs, deposition of Fe<sub>3</sub>O<sub>4</sub> NPs on surface of a pre-synthesized PANI and one-step

chemical oxidative polymerization using metal salts as the oxidant [6]. Magnetic nanocomposites based on PANI/Fe<sub>3</sub>O<sub>4</sub> that are prepared by these methods typically showed a wide particle size distribution, containing non-uniform Fe<sub>3</sub>O<sub>4</sub> fraction in magnetic composite with aggregates of Fe<sub>3</sub>O<sub>4</sub> leading to an uncontrolled structure and irreproducible material properties. More recently, soft template assisted synthesis of nanostructures of PANI as well as Fe<sub>3</sub>O<sub>4</sub> NPs has received great attention due to a relatively simple, inexpensive and facile approach to prepare nanocomposite and it does not require post-treatment to remove the template unlike hard template, which destroys the as prepared nanostructure during the hard template removal process.

In this communication, we report the facile one-step synthesis of BTCA doped PANI/Fe<sub>3</sub>O<sub>4</sub> magnetic nanocomposite via modified co-precipitation cum the aqueous chemical

## 2. Experimental

### 2.1. Materials

Aniline, Ammonium persulphate [APS, (NH<sub>4</sub>)<sub>2</sub>S<sub>2</sub>O<sub>8</sub>] and benzene tetracarboxylic acid (BTCA) were purchased from Sigma Aldrich and used as received without any further purification. All chemicals are of analytical grade. All the required solutions were prepared using Milli-Q water with resistance greater than 18 MΩ was obtained from a Millipore Milli-Q system.

### 2.2 Preparation of BTCA doped PANI / Fe<sub>3</sub>O<sub>4</sub> nanocomposites

The BTCA doped PANI/Fe<sub>3</sub>O<sub>4</sub> nanocomposite was synthesized as follows. In a typical, 0.093 g of aniline (1M) solutions and 1M BTCA were dissolved individually in 10 ml

of Milli-Q water and then both the solutions were mixed together in a 250 ml round bottomed flask under constant stirring for an hour at 0-5 °C. Then, a pre-cooled solution of 1M aqueous ammonium persulphate was slowly added to the above under constant stirring. During the course of the reaction, the colour of the reaction mixture slowly turns from a colourless to light blue and eventually to dark green which indicate the formation of BTCA doped PANI. The reaction was allowed to proceed for 5 h at 0-5 °C before allowing it to attain room temperature to yield BTCA doped PANI. Then, 10 ml of 1M FeCl<sub>3</sub>·6H<sub>2</sub>O and 10 ml of 0.5 M FeSO<sub>4</sub>·7H<sub>2</sub>O aqueous solutions were rapidly injected into the above reaction mixture and temperature was slowly raised up to 65 °C under stirring, followed by the addition of 5 ml of 25 % ammonia solution. The colour of the reaction mixture was changes to black indicating the formation of magnetite. The reaction was preceded for 5 h until a very viscous PANI/Fe<sub>3</sub>O<sub>4</sub> NPs nanocomposite was obtained. The final product was centrifuged washed with distilled water followed by methanol and dried under vacuum at room temperature for 12 h. The same procedure has been adopted for preparation of all BTCA-doped PANI/Fe<sub>3</sub>O<sub>4</sub> NPs composites, except for varying the molar ratio of BTCA to aniline from 1:1 to 1:5.

### 2.3 Characterization

Phase indication of these samples was done by X-ray diffractometer (Siemens AXS D5005 X-ray diffractometer with Cu-K $\alpha$  radiation). Morphology was investigated by scanning electron microscope. FTIR spectra were recorded over the range of 400-4000 cm<sup>-1</sup> using a Perkin Elmer SPECTRUM 1000 FTIR Spectrometer to characterize the chemical structure of polymer. The powder samples were mixed thoroughly with potassium bromide (KBr) and pressed into transparent pellets. For UV-Visible absorption spectra the samples were dissolved in dimethylsulphoxide (DMSO) and spectra were recorded on a Shimadzu UV-Vis spectrophotometer, UV-2600. Thermogravimetric analysis was carried out using TGA, Cahn TG131 system with a heating rate of 20°C per minute under N<sub>2</sub> atmosphere.

## 3. Results and Discussion

Synthesis of BTCA doped PANI/Fe<sub>3</sub>O<sub>4</sub> magnetic nanocomposite is based on in-situ chemical polymerization of monomer aniline using ammoniumpersulfate (APS) as the oxidant in presence of a dopant acid BTCA. In addition to dopant acid, BTCA acts as soft-template due to its hydrophilic group (-COOH) and hydrophobic group and thereby BTCA can easily forms micelles in an aqueous solution and this act as nanoreactor also. With progressive polymerization, growth of tube is controlled by elongation process. The presence of excess BTCA prevents the formation of larger particles via steric hindrance and thereby producing PANI nanostructures.

Morphology of BTCA doped PANI/Fe<sub>3</sub>O<sub>4</sub> nanocomposites were investigated by SEM. SEM images of BTCA doped PANI/Fe<sub>3</sub>O<sub>4</sub> prepared at different molar ratios of BTCA to

monomer were presented in **Figure 1**. SEM images clearly reveal that the morphology of nanocomposites was critically dependent on the molar ratios of BTCA to monomer. The nanoflowers were obtained for 1:5 molar ratio of BTCA to monomer, while fiber like morphology were obtained for other molar ratios (1: 1, 1:2, 1:3, 1:4).

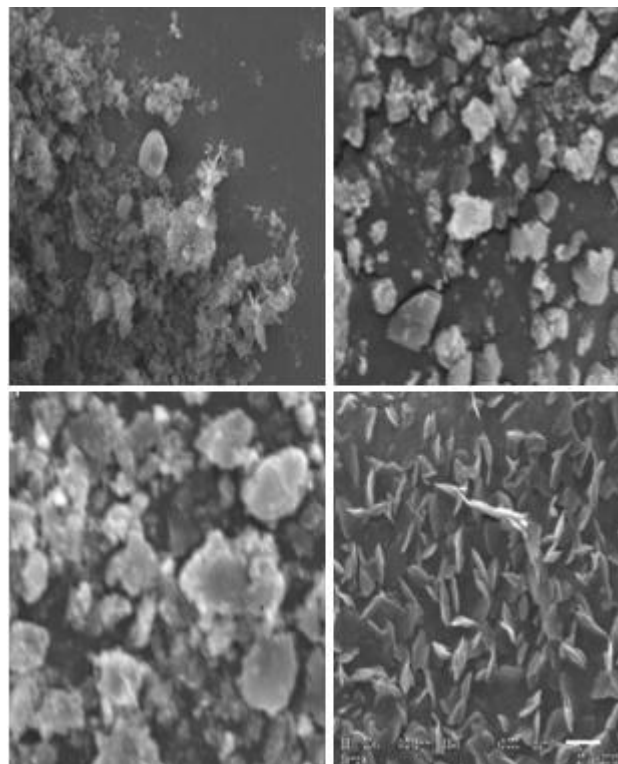


**Figure 1:** SEM images of BTCA doped PANI/Fe<sub>3</sub>O<sub>4</sub> prepared at different molar ratios of BTCA to monomer.

Molecular structure of BTCA doped PANI/Fe<sub>3</sub>O<sub>4</sub> was investigated by UV-Visible and FTIR spectroscopy and power XRD. Fig. 2 shows UV-Visible spectra of BTCA doped PANI/Fe<sub>3</sub>O<sub>4</sub> nanocomposites prepared at different molar ratios of BTCA to monomer. It can be seen from the Fig. 3 that there are two characteristic peaks centred at 320 and 610 nm. The peak at 320 nm is associated to the  $\pi-\pi^*$  transition in the benzenoid rings, while other peak at 610 nm is attributed to the due to transition of inter chain charge transfer from two adjacent benzenoid rings to the quinoid ring of PANI chain[7]. Blue shift of both absorption peaks as compared to those of pure PANI confirms presence of the interaction between Ferric ions with nitrogen atom of PANI.

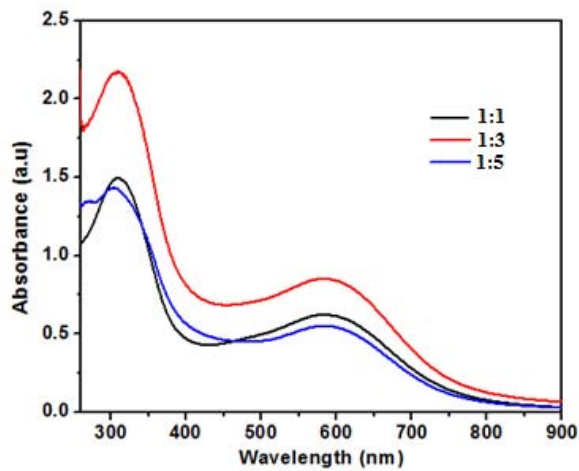


**Figure 2:** Absorption spectra of BTCA doped PANI/Fe<sub>3</sub>O<sub>4</sub> prepared at different molar ratios of BTCA to monomer.

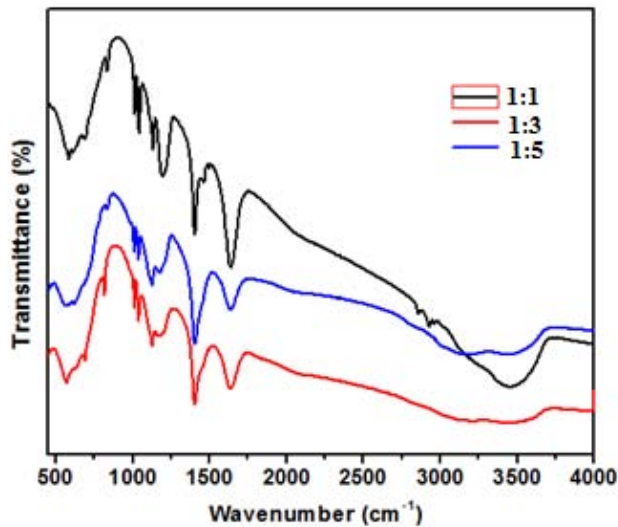


**Figure 3:** FTIR spectra of BTCA doped PANI/Fe<sub>3</sub>O<sub>4</sub> prepared at different molar ratios of BTCA to monomer.

FTIR spectra of the BTCA doped PANI/Fe<sub>3</sub>O<sub>4</sub> samples prepared at different molar ratios of BTCA to monomer depicted in Fig.3 are in good agreement with earlier reports [8-10]. The peaks at 3,465 and 3,135 cm<sup>-1</sup> are ascribed to N-H stretching vibrations of amino groups in the structural units of the PANI, while the peaks at 1,593 and 1,498 cm<sup>-1</sup> due to quinoid rings and benzenoid ring units. The presence of these peaks confirms the PANI is composed of both amine and the imine units. The peak at 1,402 cm<sup>-1</sup> is ascribed to stretching frequency of B-N = Q moiety (where B refers to benzenoid phenyl rings and Q refers to quinoid phenyl ring) and confirms the presence of phenazine units. The peaks at 1,303 cm<sup>-1</sup> corresponds to C-N stretching vibration mode of the 1, 4-disubstituted benzene ring of PANI, while the peaks at 1,170 cm<sup>-1</sup> attributed to N=Q=N modes of PANI. The peak at 828 cm<sup>-1</sup> can be attributed to the characteristic C-H out of plane bending of 1, 4-disubstituted benzene rings of PANI. The characteristic peaks at 562 and 427 cm<sup>-1</sup> were due to the intrinsic Fe-O vibrations of tetrahedral and octahedral Fe<sup>3+</sup>,

respectively [11]. FTIR results confirm that ferric ion is coordinated with the nitrogen atom of quinine rings of PANI. The power XRD patterns of BTCA doped PANI/Fe<sub>3</sub>O<sub>4</sub> nanocomposites depicted in Fig.4, consists of two broad peaks at 2 θ = 22 ° and 25 ° that can be ascribed to the periodicity parallel and perpendicular to the polymer chain of PANI. The diffraction patterns centered at 2 θ = 30 °, 35 °, 43 °, 56.22 °, 62 °, could be indexed as (220), (311), (400), (511), and (440) planes of magnetite (JCPD file No. 19-0629) [12].

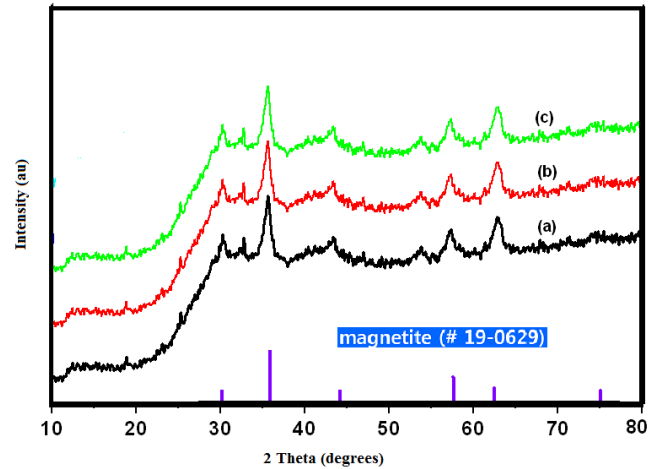


**Figure 4:** Power XRD patterns of BTCA doped PANI/Fe<sub>3</sub>O<sub>4</sub> prepared at different molar ratios of BTCA to monomer.

The room temperature magnetization curve of BTCA doped PANI/Fe<sub>3</sub>O<sub>4</sub> nanocomposites is presented in Fig. 5 The magnetization curves shows superparamagnetism of BTCA doped PANI/Fe<sub>3</sub>O<sub>4</sub> as there are no hysteresis loops with remanence and coercivity. Saturation magnetization (Ms) values 55, 37, 14 and 7 emu/g were obtained for the samples with 1:1, 1:3, and 1:5 molar ratios of BTCA to monomer. The decrease in Ms values with respect to bulk Fe<sub>3</sub>O<sub>4</sub> (Ms = 92 emu/g) is attributed to the finite size effect, surface effect and non-magnetic BTCA [13].

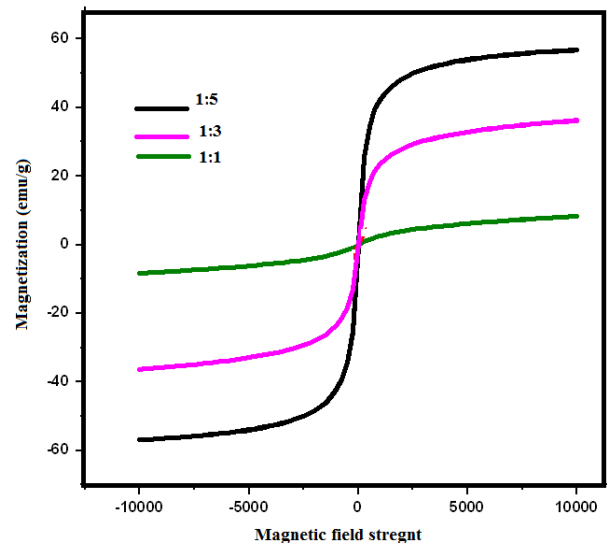


**Figure 5:** Room temperature magnetization curves of BTCA doped PANI/Fe<sub>3</sub>O<sub>4</sub> prepared at different molar ratios of BTCA to monomer.

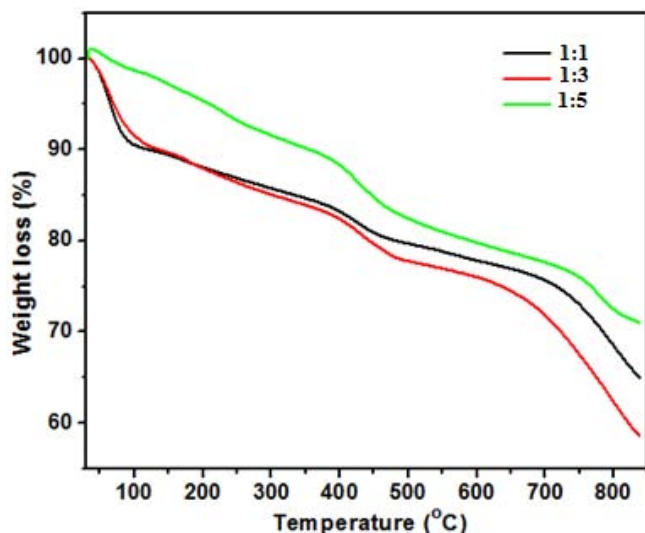


**Figure 6:** Representative TGA curves of BTCA doped PANI/Fe<sub>3</sub>O<sub>4</sub> prepared at different molar ratios of BTCA to monomer

The thermogravimetric curves for pure PANI and BTCA doped PANI/Fe<sub>3</sub>O<sub>4</sub> nanocomposites under nitrogen atmosphere at a heating rate 20 °C/min in the temperature range of 40–850 °C were depicted in Fig.6. Three weight loss steps were observed for pure PANI as well as for BTCA doped PANI/Fe<sub>3</sub>O<sub>4</sub> nanocomposite. The first weight loss up to 145 °C is ascribed to the loss of water and excess of unbound BTCA. The second weight loss between 145 and 350 °C is associated to degradation of the bound BTCA. The final weight loss between 500 and 850 °C corresponds to degradation of PANI. Higher thermal stability of nanocomposites as compared to pure PANI may be explained based on the interaction between PANI and Fe<sub>3</sub>O<sub>4</sub> NPs, which restricts the thermal motion of PANI chain in the nanocomposite.

#### 4. Conclusions

We have demonstrated a simple and reproducible one-pot synthesis of PANI nanowire containing Fe<sub>3</sub>O<sub>4</sub> NPs using APS as an oxidant in presence of BTCA as surfactant via in situ self-assembly method. The spectroscopic and microscopic techniques indicated that Fe<sub>3</sub>O<sub>4</sub> NPs are decorated on surfaces of PANI nanowires. Morphology and magnetic properties of nanocomposites were found to be critically dependent on the molar ratios of BTCA to monomer. Magnetic measurements indicated the formation of single domain particles that exhibited superparamagnetism. Thermal studies indicated that the thermal stability of nanocomposite is higher as compared to pure PANI.

#### 5. Acknowledgments

Authors are gratefully acknowledged the financial support of the University Grant commission (UGC-India), India.

#### References

- [1] Gangopadhyay, R. and De, A. (2000). Conducting Polymer Nanocomposites: A Brief Overview. *Chemistry of Materials*, 12 (3): 608-622.
- [2] Xie, N., Jiao, Q. J. and Zang, C. G. (2008). The Influence of Surface Modification of Multi-Walled Carbon Nanotubes on the Electrical Property of its Polyethylene Composite. *Advanced Materials Research*, 47–50, 1145-1148.
- [3] Fang, F. F., Lee, B. M. and Choi, H. J. (2010). Electrorheologically intelligent polyaniline and its composites. *Macromolecular Research*, 18 (2); 99-112.
- [4] Barber, P., Balasubramanian, S., Anguchamy, Y., Gong, S., Wibowo, A., Gao, H., Ploehn, H. J. and Loye, H. (2009). Polymer Composite and Nanocomposite Dielectric Materials for Pulse Power Energy Storage. *Materials*, 2(4): 1697-1733.
- [5] Raj, K., Moskowitz, B. and Casciari, R. (1995). Advances in ferrofluid technology. *Journal of Magnetism and Magnetic Materials*, 149 (1-2): 174-180.
- [6] Xuan, S., Wang, Y.-X. J., Yu, J. C. and Leung, K. C.-F. (2009). Preparation, Characterization, and Catalytic Activity of Core/Shell Fe<sub>3</sub>O<sub>4</sub>@Polyaniline@Au Nanocomposites. *Langmuir*, 25 (19): 11835–11843.
- [7] Hasik M, Kurkowska I and Bernasik A. (2006). Polyaniline incorporating cobalt ions from CoCl<sub>2</sub> solutions. *Reactive and Functional Polymers*, 66 (12): 1703-1710.
- [8] Chen, S. A. and Lee, H. T. (1993). Polyaniline Plasticized with 1-Methyl-2-pyrrolidone: Structure and Doping Behavior. *Macromolecules*, 26 (13): 3254-3261.
- [9] Trhcova, M., Stejskal, J. and Prokes, J. (1999). Infrared spectroscopic study of solid-state protonation and oxidation of polyaniline. *Synthetic Metals*, 101 (1-3): 840-841.
- [10] Neoh, K. G., Pun, M. Y., Kang, E. T. and Tan, K. L. (1995). Polyaniline treated with organic acids: doping characteristics and stability. *Synthetic Metals*, 73 (15): 209–215.
- [11] Waldron, R. D. (1955). Infrared spectra of ferrites. *Physical Review*, 99 (6): 1727–1735.
- [12] Zang, L., Wan, M. and Wei, Y. (2006). Nanoscaled polyaniline fibers prepared by ferric chloride as an oxidant. *Macromolecular Rapid Communications*, 27: 366–371.
- [13] Gee, S. H, Hong, Y. K, Erickson, D. W. and Park, M. H. (2003). Synthesis and aging effect of spherical magnetite (Fe<sub>3</sub>O<sub>4</sub>) nanoparticles for biosensor applications. *Journal of Applied Physics*, 93 (10): 7560-7562.